

# Allosteric Regulation of Tryptophan Synthase Channeling: The Internal Aldimine Probed by *trans*-3-Indole-3'-acrylate Binding<sup>†</sup>

Patricia Casino,<sup>‡,§</sup> Dimitri Niks,<sup>‡</sup> Huu Ngo,<sup>‡</sup> Peng Pan,<sup>‡</sup> Peter Brzovic,<sup>‡,||</sup> Lars Blumenstein,<sup>‡</sup> Thomas Reinier Barends,<sup>‡</sup> Ilme Schlichting,<sup>‡</sup> and Michael F. Dunn<sup>\*,‡</sup>

Department of Biochemistry, University of California, Riverside, California 92521, and Department of Biomolecular Mechanisms, Max Planck Institute for Medical Research, Heidelberg, Germany

Received February 25, 2007; Revised Manuscript Received April 17, 2007

**ABSTRACT:** Substrate channeling in the tryptophan synthase bienzyme complex from *Salmonella typhimurium* is regulated by allosteric interactions triggered by binding of ligand to the  $\alpha$ -site and covalent reaction at the  $\beta$ -site. These interactions switch the enzyme between low-activity forms with open conformations and high-activity forms with closed conformations. Previously, allosteric interactions have been demonstrated between the  $\alpha$ -site and the external aldimine,  $\alpha$ -aminoacrylate, and quinonoid forms of the  $\beta$ -site. Here we employ the chromophoric L-Trp analogue, *trans*-3-indole-3'-acrylate (IA), and noncleavable  $\alpha$ -site ligands (ASLs) to probe the allosteric properties of the internal aldimine, E(Ain). The ASLs studied are  $\alpha$ -D,L-glycerol phosphate (GP) and D-glyceraldehyde 3-phosphate (G3P), and examples of two new classes of high-affinity  $\alpha$ -site ligands, *N*-(4'-trifluoromethoxybenzoyl)-2-aminoethyl phosphate (F6) and *N*-(4'-trifluoromethoxybenzenesulfonyl)-2-aminoethyl phosphate (F9), that were previously shown to bind to the  $\alpha$ -site by optical spectroscopy and X-ray crystal structures [Ngo, H., Harris, R., Kimmich, N., Casino, P., Niks, D., Blumenstein, L., Barends, T. R., Kulik, V., Weyand, M., Schlichting, I., and Dunn, M. F. (2007) Synthesis and characterization of allosteric probes of substrate channeling in the tryptophan synthase bienzyme complex, *Biochemistry* 46, 7713–7727]. The binding of IA to the  $\beta$ -site is stimulated by the binding of GP, G3P, F6, or F9 to the  $\alpha$ -site. The binding of ASLs was found to increase the affinity of the  $\beta$ -site of E(Ain) for IA by 4–5-fold, demonstrating for the first time that the  $\beta$ -subunit of the E(Ain) species undergoes a switching between low- and high-affinity states in response to the binding of ASLs.

The channeling of substrate indole between the  $\alpha$ - and  $\beta$ -subunits of the tryptophan synthase bienzyme complex is subject to allosteric regulation that is controlled by the binding of substrate and/or product to the  $\alpha$ -site, covalent transformations of intermediates at the  $\beta$ -site, and the binding of a monovalent cation to the  $\beta$ -subunit at a site adjacent to, but distinct from, the  $\beta$ -catalytic site. The allosteric behavior of tryptophan synthase has been the subject of previous investigations by several laboratories (1–33). The determination of the three-dimensional structures of tryptophan synthase complexes (21, 28, 34–39) provides an important structural context for the understanding of this allostery.

Tryptophan synthase catalyzes the final two steps in the biosynthesis of L-Trp (Scheme 1A–C) (8, 16, 22, 40, 41). The first of these steps occurs at the catalytic site of the  $\alpha$ -subunit ( $\alpha$ -reaction), wherein 3-indole-D-glycerol 3'-

phosphate (IGP)<sup>1</sup> is cleaved to give indole and D-glyceraldehyde 3-phosphate (G3P) (Scheme 1A). The second step (Scheme 1B) occurs at the catalytic site of the  $\beta$ -subunit and involves the conversion of L-serine (L-Ser) and indole to L-tryptophan (L-Trp) and a water molecule. This transformation takes place in two stages [stages I and II of the  $\beta$ -reaction (see ref 42)]. Stage I of this transformation involves the elimination of the  $\beta$ -hydroxyl group of L-Ser to give the  $\alpha$ -aminoacrylate Schiff base intermediate, E(A–A). Stage

<sup>1</sup> Abbreviations:  $\alpha_2\beta_2$ , native form of tryptophan synthase from *S. typhimurium*;  $\alpha$ ,  $\alpha$ -subunit;  $\beta$ ,  $\beta$ -subunit; E(Ain), internal aldimine (Schiff base) intermediate; E(Aex<sub>1</sub>), external aldimine intermediate formed between the PLP cofactor and L-Ser; E(GD), gem diamine species; E(A–A),  $\alpha$ -aminoacrylate Schiff base; E(Q<sub>3</sub>), quinonoid intermediate that accumulates during the reaction between E(A–A) and indole; E(Q<sub>aniline</sub>), quinonoid species derived from the reaction of aniline with E(A–A); E(Aex<sub>2</sub>), L-Trp external aldimine intermediate; PLP, pyridoxal 5'-phosphate; IGP, 3-indole-D-glycerol 3'-phosphate; GP,  $\alpha$ -D,L-glycerol phosphate; G3P, D-glyceraldehyde 3-phosphate; IA, *trans*-3-indole-3'-acrylate anion; ASL,  $\alpha$ -site ligand; F6, *N*-(4'-trifluoromethoxybenzoyl)-2-aminoethyl phosphate; F9, *N*-(4'-trifluoromethoxybenzenesulfonyl)-2-aminoethyl phosphate; ANS, 8-anilino-1-naphthalene sulfonate; TEA, triethanolamine; MVC, monovalent cation;  $1/\tau_n$ , apparent first-order rate constant of the  $n$ th relaxation;  $A_n$ , amplitude of the  $n$ th relaxation;  $K_{Dapp}$ , apparent dissociation constant; SWSF, single-wavelength stopped-flow. Structural elements of tryptophan synthase are designated as follows: loop  $\alpha$ L2,  $\alpha$ 53–60; loop  $\alpha$ L6,  $\alpha$ 179–193; helix  $\alpha$ H8,  $\alpha$ 249–265; COMM domain,  $\beta$ 102–189; helix  $\beta$ H5,  $\beta$ 145–150; helix  $\beta$ H6,  $\beta$ 165–181.

<sup>†</sup> Supported by Deutsche Forschungsgemeinschaft (I.S.) and NIH Grant R01 GM55749 (M.F.D.).

\* To whom correspondence should be addressed: Department of Biochemistry, University of California, Riverside, CA 92521. Phone: (951) 827-4235. Fax: (951) 827-4434. E-mail: michael.dunn@ucr.edu.

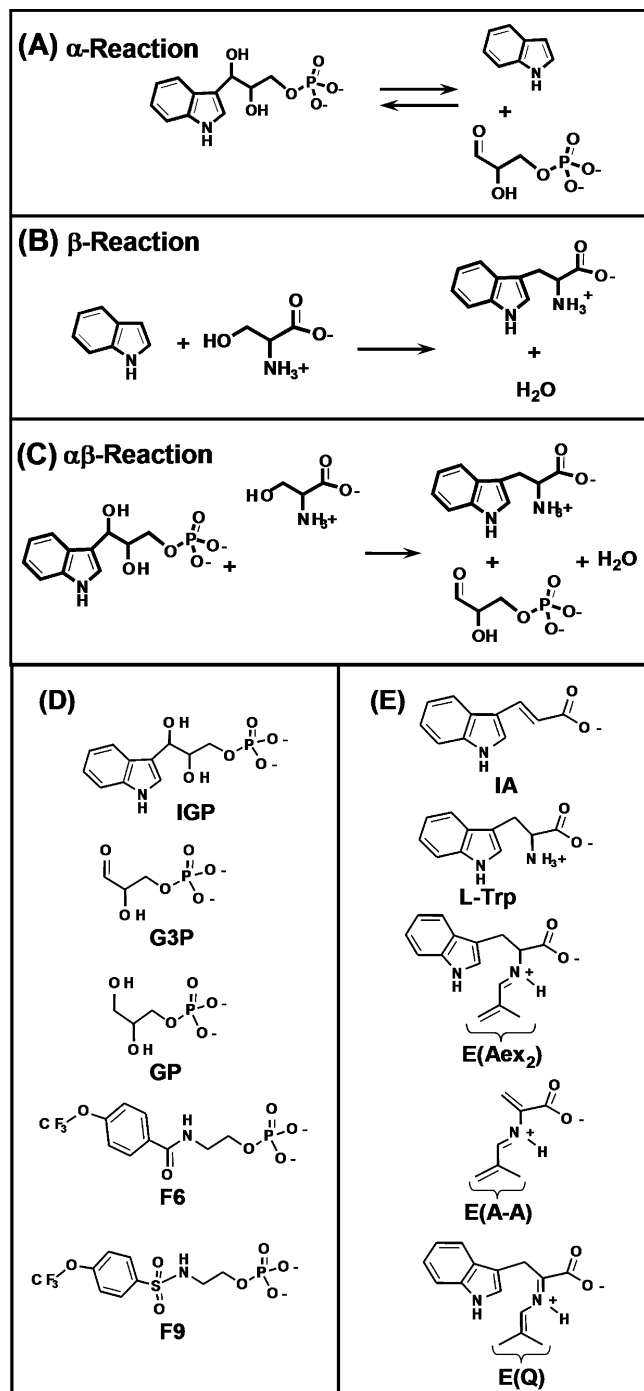
<sup>‡</sup> University of California.

<sup>§</sup> Present address: Biomedical Institute, University of Valencia, Valencia, Spain.

<sup>||</sup> Present address: Department of Biochemistry, University of Washington, Seattle, WA 98195.

<sup>‡</sup> Max Planck Institute for Medical Research.

Scheme 1:  $\alpha$ -Reaction (A),  $\beta$ -Reaction (B), and  $\alpha\beta$ -Reaction (C), (D) Comparison of the Structure of IGP with the Structures of the  $\alpha$ -Site Ligands Used in This Study, and (E) Comparison of the Structure of IA with the Structures of Key Intermediates and the Product in the  $\beta$ -Reaction



II involves transfer of the indole molecule produced at the  $\alpha$ -site to the  $\beta$ -site via the interconnecting 25 Å long tunnel where the reaction with E(A–A) occurs to give L-Trp (4, 34). The  $\beta$ -reaction pathway involves at least nine covalent intermediates formed with pyridoxal 5-phosphate (PLP) (see ref 42). The overall conversion of IGP and L-Ser to L-Trp and a water molecule, the  $\alpha\beta$  reaction, is shown in Scheme 1C. Channeling in the tryptophan synthase system is rendered efficient via a finely tuned set of allosteric interactions that function both to synchronize the catalytic activities of the  $\alpha$ - and  $\beta$ -sites and to prevent the escape of indole by

switching the  $\alpha$ - and  $\beta$ -subunits between open conformations of low activity and closed conformations of high activity (4, 7, 9–12, 16–19, 26, 28).

Despite the wealth of data available, the dynamics of the allosteric conformational changes are only partially understood in the tryptophan synthase system. Therefore, in this study, we undertake the investigation of the mechanism by which the  $\alpha$ -site substrate G3P and substrate analogues GP, F6, and F9 (42) (Scheme 1D) function as allosteric effectors using a chromophoric probe, *trans*-3-indole-3'-acrylate (IA) (Scheme 1E), which binds to the internal aldimine, E(Ain), form of the enzyme. The rapid conversion of IGP to indole and G3P at the  $\alpha$ -site makes it difficult to directly investigate the allosteric interactions arising from the binding of IGP. For these reasons, we use noncleavable analogues of IGP as probes of  $\alpha$ – $\beta$  allosteric interactions that exhibit relatively high affinity for the  $\alpha$ -site and interesting allosteric effects on the  $\beta$ -site (see refs 42 and 43) (Scheme 1D). IA shares structural features in common with  $\beta$ -site intermediates and with the product, L-Trp (Scheme 1E). As will be shown, when IA is bound to the  $\beta$ -site, its spectroscopic properties are altered by allosteric interactions arising from the binding of effectors and/or substrate analogues to the  $\alpha$ -site, providing a sensitive spectroscopic probe of ASL-mediated allosteric interactions. In this work, we report the first evidence of allosteric interactions in the internal aldimine form of the enzyme and we investigate the mechanism of these ASL-mediated allosteric transitions.

## MATERIALS AND METHODS

**Materials.** *trans*-3-Indole-3'-acrylic acid (IA) was purchased from Aldrich and used without further purification. All other materials were purchased and/or prepared as described by Ngo et al. (42).

Purification of wild-type tryptophan synthase from *Salmonella typhimurium* was performed as previously described (18, 44). All experiments in solution were carried out at 25.0  $\pm$  2  $^{\circ}$ C in the presence of 100 mM NaCl in 50 mM TEA buffer (pH 7.80) to ensure maintenance of the enzyme in the Na<sup>+</sup> form (17).

**Static and Rapid Kinetic UV–Vis Absorbance and CD Measurements and Equilibrium Binding Measurements.** Absorbance spectra and activity measurements were performed on a Hewlett-Packard 8452 diode array spectrophotometer at 25  $\pm$  2  $^{\circ}$ C. The  $\epsilon_{314}$  of IA was determined to be 1.73  $\times$  10<sup>4</sup> M<sup>–1</sup> cm<sup>–1</sup> at pH 7.8 in 50 mM TEA buffer at 25.0  $^{\circ}$ C. Circular dichroism (CD) measurements were performed on a Jobin-Yvon Dichrograph Mark V. Single-wavelength stopped-flow (SWSF) measurements were performed and analyzed as previously described (18, 19, 42). Kinetic time courses were fitted by nonlinear least-squares regression analysis using Peakfit (version 4, Jandel Scientific) to a sum of exponentials (eq 1):

$$A_t = A_{\infty} \pm \sum A_i \exp(t/\tau_i) \quad (1)$$

where  $A_t$  is the absorbance at time  $t$ ,  $A_{\infty}$  is the final absorbance,  $A_i$  is the absorbance due to the  $i$ th relaxation, and  $1/\tau_i$  corresponds to the observed rate for the  $i$ th relaxation.

Equilibrium binding studies were performed as described by Ngo et al. (42).

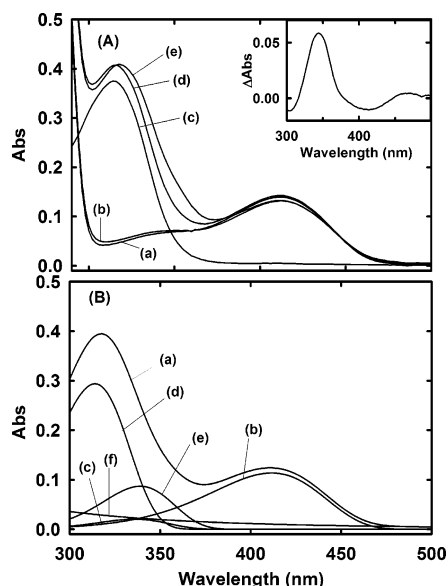


FIGURE 1: UV-vis spectra and difference spectra showing the influence of GP on the spectrum of IA. (A) Static absorption spectra for (a) 8.5  $\mu\text{M}$   $\alpha_2\beta_2$ , (b) 8.5  $\mu\text{M}$   $\alpha_2\beta_2$  and 50.0 mM GP, (c) 21.7  $\mu\text{M}$  IA and 50.0 mM GP, (d) 8.5  $\mu\text{M}$   $\alpha_2\beta_2$  and 21.7  $\mu\text{M}$  IA, and (e) 8.5  $\mu\text{M}$   $\alpha_2\beta_2$ , 21.7  $\mu\text{M}$  IA, and 50.0 mM GP. Under these conditions, the IA binding sites are only partially occupied. The difference spectrum calculated as spectrum e minus spectrum d (inset) shows the influence of GP on the spectrum of bound IA. (B) Decomposition of the absorption spectrum via lognormal fitting. The curves are as follows: (a) observed spectrum of 8.5  $\mu\text{M}$   $\alpha_2\beta_2$ , 21.7  $\mu\text{M}$  IA, and 50.0 mM GP, (b and c) lognormal curves representing bands originating from the coenzyme, (d) free IA, (e) bound IA with a  $\lambda_{\text{max}}$  of 341 nm, and (f) Rayleigh scatter curve.

## RESULTS

**UV-Vis Spectroscopic Properties of the Complexes of IA with E(Ain).** To investigate the interaction of IA with the tryptophan synthase holoenzyme complex, UV-vis absorbance spectra, CD spectra, and fluorescence emission spectra were examined for evidence of binding, both in the presence and in the absence of ASLs. Under the conditions shown in Figure 1, and in the absence of an ASL, the careful evaluation of spectra and difference spectra (data not shown) indicated there appears to be no significant change in the absorption spectrum of either IA or E(Ain) upon mixing.

When the spectrum of the enzyme mixed with IA is examined under conditions where the  $\alpha$ -site of E(Ain) is occupied by one of the ASLs investigated in this study (G3P, GP, F6, or F9), the absorbance spectrum of IA is altered and the extinction coefficient of the 412 nm band of E(Ain) is slightly decreased, indicating that IA binds under these conditions and slightly perturbs the spectrum of the internal aldimine chromophore. Figure 1 shows typical UV-vis spectra documenting the absorbance changes that occur when IA binds to the E(Ain) complexes with GP (panels A and B). Similar spectral changes occur with G3P, F6, and F9 (data not shown). In Figure 1B, the spectrum of the complex of IA with (GP)E(Ain) (component a) has been decomposed into three components (components b, c, and e) plus the light scattering curve (component f) using lognormal distribution curve fits and the spectrum of free IA (component d) (3, 17, 45). Components b and c were assigned to bands from the coenzyme. This fitting gives the predicted spectrum of bound IA as component e, with a  $\lambda_{\text{max}}$  of  $341 \pm 3$  nm. In each of

the ASL systems that were investigated [GP (Figure 1A) and G3P, F6, and F9 (data not shown)], the spectrum of bound IA is red-shifted relative to that of unbound IA; the difference spectra (bound minus unbound) have similar shapes, and each exhibits a maximum at  $\sim 343$  nm and a broad minimum at  $\sim 412$  nm. No evidence from UV-vis absorption spectra was found for the binding of IA to the GP complex of E(A-A) (data not shown), indicating that the reaction of L-Ser with the E(Ain) complex with both GP and IA bound, designated as (GP)E(Ain)(IA), gives (GP)E(A-A) with the displacement of IA.

While there is no obvious change in the absorption spectrum of IA when IA is mixed with E(Ain) in the absence of ASLs, Figure 2A shows the appearance of a new CD band in the 320–370 nm region attributable to a weak binding interaction between E(Ain) and IA. The difference spectrum (Figure 2B) shows the new band exhibits a  $\lambda_{\text{max}}$  of  $\sim 360$  nm, and there is an indication of a slight perturbation of the 412 nm CD band of E(Ain) in the presence of IA, causing a very weak minimum at  $\sim 460$  nm and the hint of a shoulder in the 410 nm region. CD measurements carried out with GP bound to the  $\alpha$ -site (Figure 2C,D) give changes in the CD spectrum attributable to bound IA that are similar to those observed in the absence of an ASL, but indicative of a slightly tighter interaction. However, the CD band attributable to IA is shifted, and the difference spectrum exhibits a maximum at a  $\lambda_{\text{max}}$  of 345 nm. Again, IA binding appears to slightly perturb the CD band arising from the 412 nm absorption band of the E(Ain) chromophore. These experiments indicate that both in the presence and in the absence of GP, the binding of IA gives rise to a new set of induced CD transitions due to the chiral microenvironment of the bound IA chromophore, and to perturbations of the PLP CD band. The dependence of the amplitude of the 410 nm band on the concentration of IA (data not shown) indicates the binding interaction is relatively weak, both in the absence and in the presence of an  $\alpha$ -site ligand. Because of the strong absorbance background contributed by unbound IA, meaningful measurements could not be made at IA concentrations above  $\sim 60$   $\mu\text{M}$ , and therefore, the CD data could not be used to quantify binding affinity.

The binding of IA to E(Ain) was further investigated by quantifying the influence of IA on either the fluorescence of the internal aldimine chromophore or the fluorescence of the binding probe, 8-anilino-1-naphthalenesulfonate, ANS (15). Excitation of the 412 nm absorption band of E(Ain) gives a weak fluorescence emission with a  $\lambda_{\text{max}}$  of 490 nm (spectra not shown) (40, 41). In the absence of  $\alpha$ -site ligands, the addition of IA to solutions of E(Ain) caused quenching of this fluorescence but did not shift the position of the emission maximum (60.0  $\mu\text{M}$  IA gave  $\sim 20\%$  quenching). Analyses assuming a simple binding equation (42) (Materials and Methods) gave the apparent dissociation constants listed in Table 1. As summarized in Table 1, the concentration dependence of this quenching indicates that in the absence of an  $\alpha$ -site ligand, IA binds very weakly to E(Ain).

The work of Pan and Dunn (15) established that ANS is a sensitive fluorescence probe of ligand-induced conformational changes in the tryptophan synthase system. They showed that when bound to the enzyme, ANS is strongly fluorescent, whereas when ANS is free in an aqueous solution, its fluorescence is nearly completely quenched. The

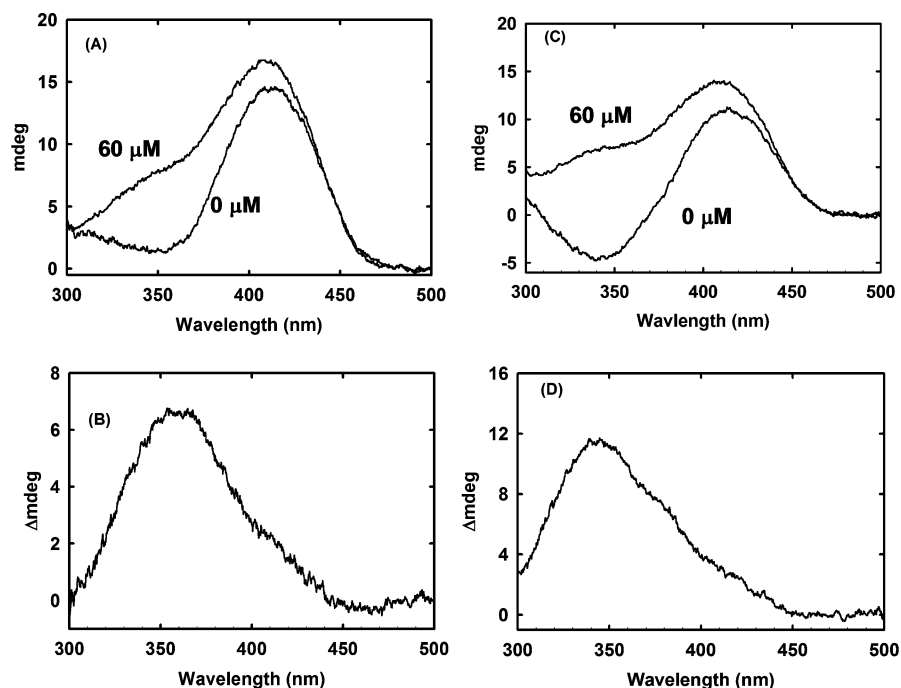


FIGURE 2: Circular dichroism (CD) spectra (A and C) and difference spectra (B and D) of 10  $\mu\text{M}$   $\alpha_2\beta_2$  in the presence of 60  $\mu\text{M}$  IA (A and B) or in the presence of 60  $\mu\text{M}$  IA and 50 mM GP (C and D). Measurements were performed at 25  $^{\circ}\text{C}$  in 50 mM TEA buffer (pH 7.80).

Table 1: Summary of Apparent Dissociation Constants Determined by Fluorescence

enzyme and ligand incubation conditions	ligand that was varied	$K_{\text{Dapp}}$ (mM) <sup>a</sup> ( $\lambda_{\text{ex}}$ = 410 nm)	$K_{\text{Dapp}}$ (mM) <sup>b</sup> ( $\lambda_{\text{ex}}$ = 380 nm)
E(Ain)	IA	$0.86 \pm 0.2$	$0.92 \pm 0.2$
E(Ain) with 50 mM GP	IA	$0.169 \pm 0.03$	$0.252 \pm 0.04$
E(Ain) with 0.4 mM F9	IA	$0.195 \pm 0.05$	$0.298 \pm 0.05$
E(Ain) with 1.0 mM F6	IA	$0.74 \pm 0.2$	$0.41 \pm 0.2$
E(Ain)	GP		$11.4 \pm 1^c$
E(Ain) with 60 $\mu\text{M}$ IA	GP	$17.7 \pm 3$	$11.4 \pm 3$
E(Ain)	F9		$0.050 \pm 0.005^c$
E(Ain) with 60 $\mu\text{M}$ IA	F9		$0.158 \pm 0.03$
E(Ain)	F6		$0.280 \pm 0.05^c$
E(Ain) with 60 $\mu\text{M}$ IA	F6		$0.637 \pm 0.06$
E(Ain)	G3P		$4.1 \pm 1^d$

<sup>a</sup> Signal derived from the fluorescence of E(Ain). <sup>b</sup> Signal derived from the fluorescence of ANS. <sup>c</sup> Values taken from ref 42. <sup>d</sup> Concentration corrected for hydration of G3P (42).

binding of ligands to either the  $\alpha$ -site or the  $\beta$ -site was found to weaken the affinity of the enzyme for ANS, causing attenuation of the fluorescence signal because of the decrease in the level of bound ANS. The ANS fluorescence study presented in Figure 3 shows that when F9 is bound to the enzyme, the binding of IA also decreases the fluorescence of ANS, presumably via a decrease in the amount of ANS bound. Similar results were found for F6 and G3P (data not shown). When fit to a hyperbolic binding equation (42), the resulting changes in ANS fluorescence provide a measure of the apparent affinity of IA for the enzyme. Analyses of the concentration dependencies of the ANS fluorescence signals (Table 1) indicate that the binding of ASLs has a synergistic effect on the affinity of IA for the enzyme. Consequently, the binding of GP, G3P, F9, or F6 was found to strengthen the binding of IA.

**Kinetics of the Reaction of IA with the GP, G3P, F9, or F6 Complexes of E(Ain).** Figure 4 shows representative time courses for the shift in the spectrum of IA upon formation of the ternary complex with (GP)E(Ain) at two different

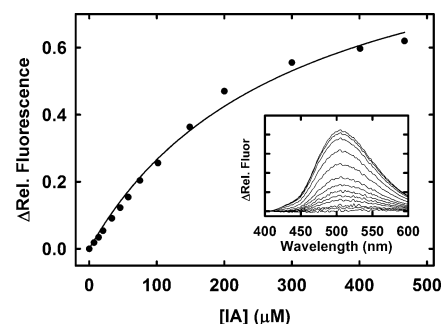


FIGURE 3: Isotherm showing the absolute value of the decrease in ANS fluorescence ( $\lambda_{\text{ex}}$  = 360 nm) when IA binds to the (F9) $\alpha_2\beta_2$  complex. [ $\alpha_2\beta_2$ ] = 10  $\mu\text{M}$ ; [F9] = 4 mM, and [IA] was varied from 0 to 470  $\mu\text{M}$ . The solid line represents the best fit to a hyperbolic expression with an apparent dissociation constant for IA of  $0.298 \pm 0.03$  mM. The inset shows difference spectra for the decrease in ANS fluorescence as [IA] is varied. The residual ANS fluorescence at 470  $\mu\text{M}$  IA has been subtracted from each trace.

concentrations of GP (panel A) or two different concentrations of IA (panel B). These time courses are all fitted well by the equation for a single relaxation (eq 1, where  $i = 1$ ). The kinetics of the IA spectral changes for formation of the complexes with (G3P)E(Ain), (F9)E(Ain), and (F6)E(Ain) (data not shown) all exhibited kinetic behavior similar to that of the (GP)E(Ain) system. The time-resolved spectral changes measured by rapid-scanning stopped-flow (RSSF) UV-vis spectrophotometry (data not shown) for the reaction of IA with the (GP)E(Ain) complex were fully consistent with a single-exponential process.

Figures 5 and 6 summarize the rate and amplitude data for the time courses resulting from the IA spectral changes measured as described in panels A and B of Figure 4 for the GP, F9, F6, and G3P systems. Panels A, C, E, and G of Figure 5 compare the dependencies of  $1/\tau$  for the reactions of IA with (GP)E(Ain), (F9)E(Ain), (F6)E(Ain), and (G3P)E(Ain), respectively, on the concentration of the ASL (GP,



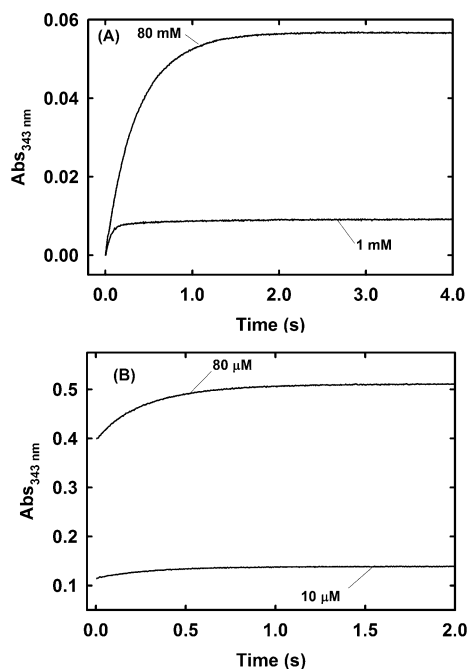


FIGURE 4: Typical SWSF time courses for the appearance of the red-shifted spectra of ternary complexes formed among IA, GP, and  $\alpha_2\beta_2$ . (A) Reaction of  $(GP)\alpha_2\beta_2$  with IA at 1.0 and 80.0 mM GP. Conditions:  $[\alpha_2\beta_2] = 10.0 \mu\text{M}$ , and  $[IA] = 30.0 \mu\text{M}$ . (B) Reaction of  $(GP)\alpha_2\beta_2$  with IA at 10 and 80.0  $\mu\text{M}$  IA. Conditions:  $[\alpha_2\beta_2] = 10.0 \mu\text{M}$ , and  $[GP] = 50.0 \text{ mM}$ .

F9, F6, and G3P, respectively). The corresponding amplitude dependencies are shown in panels B, D, F, and H, respectively. The dependencies of  $1/\tau$  on the concentration of IA for GP are shown in Figure 6A. The corresponding amplitude dependencies are shown in Figure 6B. Because of the magnitude of the extinction coefficient of free IA in the wavelength region of interest and the optical path length used in the stopped-flow apparatus (1.00 cm), the concentration dependencies were limited to the range from  $\sim 5.0$  to  $\sim 80.0 \mu\text{M}$ .

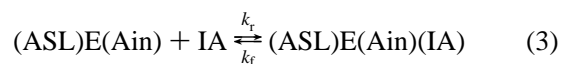
The plots of  $1/\tau$  versus the ASL concentration (Figure 5A,C,E,G) were found to sharply decrease at low concentrations and then extrapolate to a non-zero, limiting value at high concentrations. These curves were fitted well (solid lines) by the expression for a hyperbolic function of the form shown in eq 2:

$$1/\tau = (k_{\text{app}}^0 K_{\text{app}})/(K_{\text{app}} + [L]) + k_{\text{app}} \quad (2)$$

In this treatment (46), the y-intercept ( $1/\tau_0$ ) obtained from extrapolation of the curve to zero ligand concentration is given by the sum of two apparent first-order rates ( $1/\tau_0 = k_{\text{app}}^0 + k_{\text{app}}$ ). The limiting rate approached at high ligand concentrations is the apparent first-order rate,  $k_{\text{app}}$ , and the apparent hyperbolic constant for the curve is  $K_{\text{app}}$ . The values derived from the best fits of the data in Figure 5 to eq 2 for GP, F9, F6, and G3P are summarized in Table 2. Comparison of these data shows that GP, G3P, and F9 all give similar rate values. The behavior of F6 is somewhat divergent. The value of  $1/\tau$  extrapolated to high F6 concentrations appears to be significantly greater than the values obtained for GP, G3P, and F9, yielding a larger value for  $k_{\text{app}}$  ( $\sim 9.9 \text{ s}^{-1}$  vs  $\sim 2 \text{ s}^{-1}$ ). This behavior does not seem to reflect the presence of the second, weaker mode of binding<sup>2</sup> found for F6 (see ref 42).

The plots of  $1/\tau$  versus  $[IA]$  in Figure 6 for the GP system (panel A) were found to be adequately fit assuming a linear dependence (solid lines) with small, near-zero slopes, consistent either with an apparent second-order rate law or with a two-step mechanism involving a binding step linked to a unimolecular process where the binding affinity is very weak. The curve for the F9 system (data not shown) appears to give a deviation from linearity at low IA concentrations. However, if the data point measured at the lowest IA concentration is ignored (where the assumption of the pseudo-first-order approximation,  $[\text{ligand}] \gg [\text{enzyme sites}]$ , is invalid), then the remaining data points could be fitted with a linear curve with a shallow, positive slope. The plot for F6 (data not shown) was found to be adequately fit assuming a linear dependence with a slope of zero (within experimental error), implying that either the process is unimolecular or the experimental error is too large to allow detection of a shallow slope. The plot of  $1/\tau$  versus  $[IA]$  for G3P (data not shown) was found to be linear with a slope of zero (within experimental error) over the concentration range 0–50  $\mu\text{M}$  IA. At higher concentrations (50–80  $\mu\text{M}$ ), the value of  $1/\tau$  was found to decrease slightly from  $\sim 6.0$  to  $\sim 5.5 \text{ s}^{-1}$ . The dependencies of amplitude on the concentration of IA (viz., Figure 6B) in each instance showed shallow curvature corresponding to a slight increase in amplitude over the concentration range that was studied.

If it is assumed that the weak IA concentration dependencies of  $1/\tau$  (viz., Figure 6) arise from a simple, bimolecular binding mechanism, eq 3, then the y-intercept measures the IA dissociation rate,  $k_r$ , and the slope measures the formation rate,  $k_f$ .



According to this treatment, the apparent dissociation constant for IA binding,  $K_D$ , is given by the ratio  $k_r/k_f$ . Values for  $k_r$ ,  $k_f$ , and  $K_D$  calculated from the kinetic data (viz., Figure 6A) are summarized in Table 3. When fitted to a hyperbolic equation (42), the amplitude dependencies (viz., Figure 6B) all gave apparent dissociation constants,  $K'_D$ , of approximately 0.2 mM (Table 3), values in reasonable agreement with the  $K_D$  values calculated from the slope and intercept data.

**Crystal Structure of the  $(F9)\text{E}(\text{Ain})(\text{IA})$  Complex.** Crystals of tryptophan synthase were soaked with IA [10% (v/v) IA in THF] and F9 (10 mM) to determine the binding site of the chromophoric probe. The resulting complex structure exhibited a new electron density peak at the  $\beta$ -site that was attributed to the binding of IA. Our interpretation of this electron density places the IA carboxylate within the same subsite occupied by the carboxylates of the L-Ser and L-Trp external aldimines in their respective complexes (21, 28–30, 36). However, no electron density was observed for the aromatic ring and the carbon chain of the IA molecule,

<sup>2</sup> The X-ray crystallographic studies presented in ref 42 present evidence that at very high concentrations of F6, this ligand binds to two sites, the  $\alpha$ -site and an unusual site within the  $\beta$ -subunit consisting of a portion of the tunnel and the  $\beta$ -catalytic site. Since the crystallographic work indicates binding to this second site occurs only at very high F6 concentrations, we conclude that this interaction is unlikely to be important for the work described in this paper.

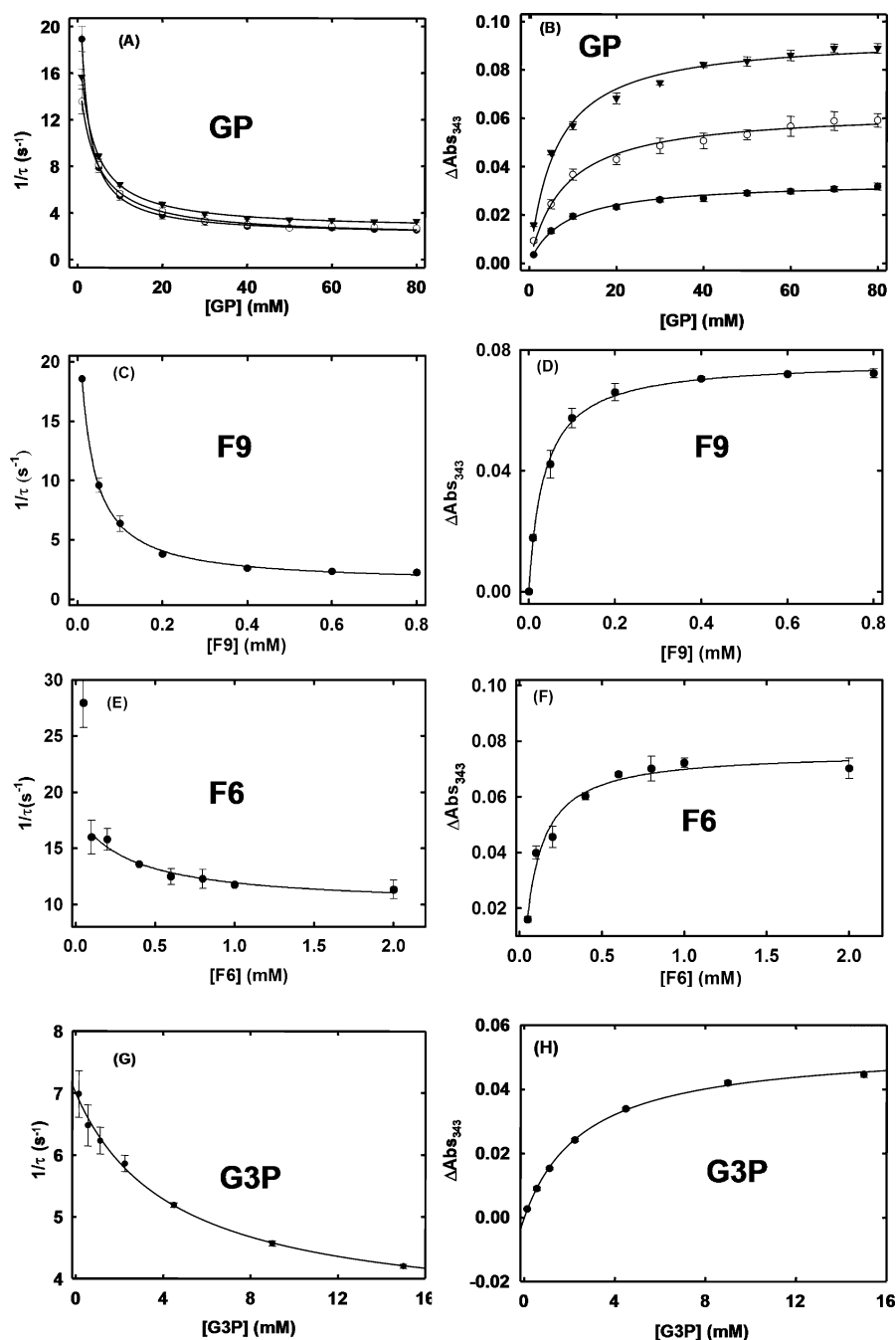


FIGURE 5: Concentration dependencies of rates ( $1/\tau$ ) and amplitudes ( $\Delta\text{Abs}_{343}$ ) of the relaxations for formation of the  $\alpha_2\beta_2$  ternary complexes of IA and ASLs. SWSF time courses were measured at the wavelength of the maximum in the difference spectrum (343 nm) by mixing  $\alpha_2\beta_2$  and IA with the ASL, or by mixing  $\alpha_2\beta_2$  and the ASL with IA. The order of preincubation of reagents ( $\alpha_2\beta_2$  with IA or with the ASL) was found to make no difference. The dependencies of  $1/\tau$  on [ASL] with [IA] held constant are as follows: GP (A), F9 (C), F6 (E), or G3P (G). The dependencies of reaction amplitude on [ASL] with [IA] held constant are as follows: GP (B), F9 (D), F6 (F), or G3P (H). (A and B)  $[\alpha_2\beta_2] = 10 \mu\text{M}$ , and [IA] = 15.0 (●), 30.0 (○), or 60.0  $\mu\text{M}$  (▼). (C and D)  $[\alpha_2\beta_2] = 30 \mu\text{M}$ , and [IA] = 30.0  $\mu\text{M}$ . (E and F)  $[\alpha_2\beta_2] = 10 \mu\text{M}$ , and [IA] = 30  $\mu\text{M}$ . (G and H)  $[\alpha_2\beta_2] = 30 \mu\text{M}$ , and [IA] = 30  $\mu\text{M}$ .

preventing unambiguous modeling of the IA complex. As the structure resembles the (F9)E(Ain) complex (42) in all other regards, the structure was neither included in this paper nor submitted to the Protein Data Bank.

## DISCUSSION

*Conformational Switching Is Central to the Regulation of Channeling in the Tryptophan Synthase Bifunctional Complex.* The solution kinetic studies of Dunn et al. (4) provided the first experimental evidence indicating that allosteric regulation of channeling in tryptophan synthase involves the

switching of  $\alpha\beta$  dimeric units between different conformational states, designated as open and closed. Subsequent work in solution (7, 9–11, 15, 16) and in the crystalline state (21, 28–30, 34–36, 38) has shown that the binding of ligands to the  $\alpha$ -site and the reaction of L-Ser at the  $\beta$ -site drive conformational transitions in favor of the closed conformations of the  $\alpha$ - and  $\beta$ -subunits. Anderson et al. (7) proposed that the formation of the E(A–A) intermediate triggers activation of the  $\alpha$ -site. The experiments of Brzovic et al. (9), Leja et al. (12), Pan and Dunn (15), and Pan et al. (16) established that the formation of the E(A–A) intermediate

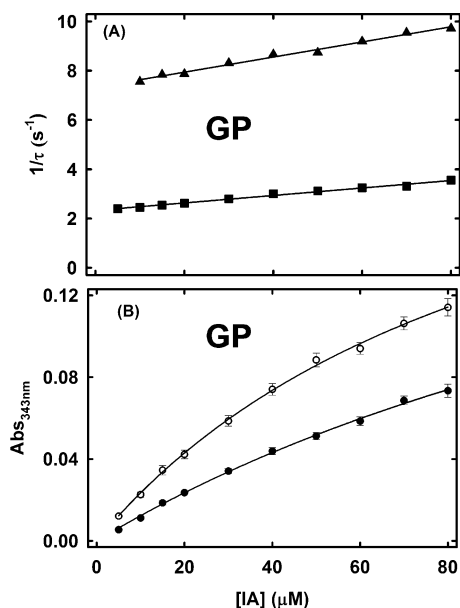


FIGURE 6: SWSF kinetics for the formation of the  $\alpha_2\beta_2$  ternary complexes of IA at two GP concentrations. Dependencies of  $1/\tau$  and reaction amplitude on [IA] are shown in panels A and B, respectively.  $[\alpha_2\beta_2] = 10 \mu\text{M}$  with 5.0 mM GP (▲) or 50.0 mM GP (■). The fittings (solid lines) are discussed in the text.

Table 2: Summary of Rate Constants and Apparent Dissociation Constants from the Data Presented in Figure 5

$\alpha$ -site ligand	$1/\tau_0^a = (k_{\text{app}}^0 + k_{\text{app}})/(K_{\text{app}} + [\text{L}])$ ( $\text{s}^{-1}$ )	$k_{\text{app}}^0$ ( $\text{s}^{-1}$ )	$k_{\text{app}}$ ( $\text{s}^{-1}$ )	$K_{\text{app}}^a$ (mM)	$K'_{\text{Dapp}}^a$ (mM)
GP with 15 $\mu\text{M}$ IA	31.5	29.4	2.07	1.15	8.07
GP with 30 $\mu\text{M}$ IA	15.1	13.2	1.95	3.33	8.02
GP with 60 $\mu\text{M}$ IA	17.9	15.4	2.55	2.71	6.04
G3P with 30 $\mu\text{M}$ IA	7.0	3.2	3.8	4.3 <sup>b</sup>	2.6 <sup>b</sup>
F9 with 30 $\mu\text{M}$ IA	23.8	22.5	1.29	0.020	0.036
F6 with 30 $\mu\text{M}$ IA	18.3	8.46	9.86	0.32	0.064

<sup>a</sup> Data from Figure 5:  $1/\tau = (k_{\text{app}}^0 K_{\text{app}})/(K_{\text{app}} + [\text{L}]) + k_{\text{app}}$ . In this treatment, the y-intercept ( $1/\tau_0$ ) obtained from extrapolation of the curve to zero ligand concentration is the sum of two apparent first-order rates ( $1/\tau_0 = k_{\text{app}}^0 + k_{\text{app}}$ ), the limiting rate approached at high ligand concentrations is the apparent first-order rate,  $k_{\text{app}}$ , and the apparent hyperbolic constant for the curve is  $K_{\text{app}}$ .  $K'_{\text{Dapp}}$  values were estimated from the dependence of the amplitude of  $1/\tau$  on ASL concentration.

<sup>b</sup> Concentration not corrected for hydration of G3P. Experimental error percentages were estimated to have the following values:  $1/\tau_0$ ,  $\pm 15\%$ ;  $k_{\text{app}}/\tau_0$ ,  $\pm 10\%$ ;  $K_{\text{app}}$ , 10%;  $K'_{\text{Dapp}}$ ,  $\pm 8\%$ .

Table 3: Summary of Rate Constants and Apparent Dissociation Constants for the Binding of IA to the ASL Complexes of E(Ain)<sup>a</sup>

$\alpha$ -site ligand	$k_t^b$ ( $\text{M}^{-1} \text{s}^{-1}$ )	$k_r^c$ ( $\text{s}^{-1}$ )	$K_D = k_r/k_t$ (mM)	$K'_D$ (mM)
GP (5 mM)	$3.3 \times 10^4$	7.2	0.22	$\sim 0.2$
GP (50 mM)	$1.9 \times 10^4$	2.2	0.12	$\sim 0.1$
G3P (2.0 mM) <sup>c</sup>		6.0		
F6 (2.0 mM)		9.7		$\sim 0.2$
F9 (0.4 mM)	$1.0 \times 10^4$	2.15	0.22	$\sim 0.2$

<sup>a</sup> Values were estimated from the data presented in Figure 6.

<sup>b</sup> Calculated as the slope of the best fit linear fitting of the data in Figure 6. <sup>c</sup> Values calculated as the y-intercept. Errors for the values of  $k_t$  and  $k_r$  are estimated to be  $\pm 15\%$ . <sup>d</sup> Values determined from the dependence of amplitude on IA concentration (see Figure 6B). <sup>e</sup> Concentration not corrected for hydration of G3P.

at the  $\beta$ -site is the trigger that activates the  $\alpha$ -site and that the conversion of E(Q) to E(Aex<sub>2</sub>) triggers deactivation of the  $\alpha$ -site. Consequently, this switching between open and closed conformations plays critically important roles in the

allosteric regulation of indole channeling by modulating the activity of the  $\alpha$ -site in response to covalent reactions at the  $\beta$ -site and by sequestering indole within the confines of the tunnel and the  $\alpha$ - and  $\beta$ -sites, thus preventing its escape. Most structures with substrates or substrate analogues bound to the  $\alpha$ -site show  $\alpha\text{Glu49}$  folded away from the position that would allow the carboxyl group to perform the acid–base catalysis needed to cleave IGP. In the active conformation,  $\alpha\text{Glu49}$  is correctly positioned to serve the dual roles of a proton at the IGP indolyl ring C3 and abstraction of a proton from the IGP 3'-hydroxyl as a bifunctional catalyst (39).

Heretofore, the discussion of conformational transitions in tryptophan synthase has considered the possibility that reciprocal interactions at the  $\beta$ -site accompany the binding of ligands to the  $\alpha$ -site (3, 4, 6, 9–11, 15, 16, 18, 19, 21, 26, 29, 30). The spectroscopic, kinetic, and structural studies presented herein provide new insights into the structure and allosteric mechanism of these site–site interactions.

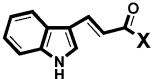
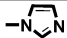
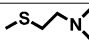
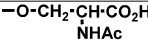
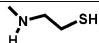
**Assignment of the IA Binding Site.** The experiments presented in this study (Figures 1–6) establish that in the presence of an ASL, the ternary complexes with E(Ain) give spectra with the  $\pi$ – $\pi^*$  transition of IA shifted from 317 nm in the unbound state to  $\sim 341$  nm in the bound state. As shown both by solution studies of ligand binding (Figures 1–6) and X-ray structures of the crystalline ligand–protein complexes (42), the ASLs used in this study (GP, G3P, F6, and F9) all bind exclusively to the  $\alpha$ -site under the conditions employed in this work.<sup>2</sup> Since inspection of these and other tryptophan synthase structures in complex with  $\alpha$ -site ligands (21, 28–30, 36, 38, 39) shows that the  $\alpha$ -site is too small to accommodate both IA and any of these ASLs simultaneously, the  $\alpha$ -catalytic site can be eliminated as the locus of IA binding in the (ASL)E(Ain)(IA) ternary complexes.

IA has structural features in common with the product, tryptophan, and with the structures of the E(A–A) and E(Q) species (see Scheme 1E). Since the reaction of L-Ser appears to displace IA from the (GP)E(Ain)(IA) complex, it follows that in all probability when the  $\alpha$ -site is occupied by an ASL, IA binds to the  $\beta$ -site of E(Ain).

This work establishes that IA binds very weakly to the  $\beta$ -site of E(Ain) in the absence of an ASL, and this binding interaction is significantly enhanced when ASLs are present (Figures 1–6 and Tables 1, 2 and 3). This conclusion is further supported by the observation that the (F9)E(Ain)-(IA) complex structure indicates a bound IA at the  $\beta$ -active site even if parts of the probe are too mobile to be observable. The spectral studies presented in this work (Figures 1–3) do not unambiguously identify the site to which IA binds in the absence of ASLs.<sup>3</sup> However, the CD band of the 412 nm absorption band of E(Ain) is similarly perturbed by IA binding both when the  $\alpha$ -site is occupied by an  $\alpha$ -site ligand and when the  $\alpha$ -site is unoccupied (Figure 2). This observation and the finding that the fluorescence emission spectrum of the PLP moiety of E(Ain) ( $\lambda_{\text{ex}} = 412$  nm) is quenched by

<sup>3</sup> In the absence of ASLs, both the  $\alpha$ - and  $\beta$ -sites of tryptophan synthase a priori are available for the binding of indole and indole derivatives such as IA. Therefore, it is not unreasonable to expect that IA binds to both sites. The spectral data presented in Figures 1–3 suggest that IA binds to the  $\beta$ -site, albeit very weakly. The data of Marabotti et al. (24) indicate that in the absence of an ASL, IA also binds to the  $\alpha$ -site.

Table 4: Dependence of the Absorption Spectral Maximum of the Indoleacrylyl Chromophore on the Nature of the Carbonyl Substituent, X

Indoleacrylyl Derivative:	-X	$\lambda_{\max}$ (nm)	Reference
			
acyl imidazole		378	(53)
thioester		365	(57)
native acyl enzyme	-O-Ser <sub>195</sub> $\alpha$ -Chymotrypsin (Native)	359	(56)
methyl ketone	-CH <sub>3</sub>	355	(47, 56)
-O (N-acetyl serine ester)		335	(47, 56)
denatured acyl enzyme	-O-Ser <sub>195</sub> $\alpha$ -Chymotrypsin (Denatured)	334	(56)
carboxylic acid	-OH	330	(56)
amide		326	(56)
carboxylate	-O <sup>-</sup>	313	(56)
complex of IA and GP with tryptophan synthase	(GP)E(Ain)(IA)	341	this work

the binding of IA (Figure 3 and Table 1) strongly indicate that IA also binds to the  $\beta$ -catalytic site in the absence of ASLs.<sup>3</sup>

**IA Spectral Change.** The arylacrylyl chromophores are sensitive optical probes of the polarity of protein sites (47–50). The arylacrylyl system has been used extensively to investigate the acyl enzymes formed with serine proteases such as  $\alpha$ -chymotrypsin (47, 51–56). Arylacrylyl homologues (57) were subsequently used to investigate the catalytic mechanisms of glyceraldehyde-3-phosphate dehydrogenase (58), alcohol dehydrogenase (48, 59–62), aldehyde dehydrogenase (49, 50), and the acyl-CoA dehydrogenases (63, 64). Relative to the absorption maximum in aqueous solution, the long wavelength  $\pi \rightarrow \pi^*$  transition of the arylacrylyl chromophore typically is red-shifted when it is inserted into a microenvironment more polar than water (Table 4). In homogeneous solution, the magnitude of the red shift correlates with the dielectric properties of the medium (47, 48). Because the distribution of electron density over the conjugated  $\pi$ -system of the arylacrylyl group is sensitive to electrostatic interactions, chromophores such as IA can be useful probes of the microenvironment of a protein binding site. For example, the absorption spectrum of *trans*-4-(*N,N*-dimethylamino)cinnamaldehyde is shifted from 398 nm in aqueous solution to 464 nm in the ternary complex formed with liver alcohol dehydrogenase and NADH (59), and replacement of NADH with NAD<sup>+</sup> further shifts the spectrum to 495 nm (61, 62). In these complexes, the aldehyde carbonyl is directly coordinated to the active site zinc ion, and the positively charged nicotinamide ring of the coenzyme is bound within van der Waals distance of the chromophore carbonyl (48, 59–62).

The UV–vis absorption spectra of ternary complexes formed with IA, the ASLs, and E(Ain) (Figure 1A), and the fitting of these spectra to lognormal curves (45) show that

the spectrum of bound IA is red-shifted by  $\sim 23$  nm (Figure 1B). This red shift suggests the ternary complexes provide a microenvironment at the IA binding site that is significantly different from that in aqueous solution at pH 7.8. The data in Table 4 show that a similar shift also occurs in aqueous solution upon protonation of the IA carboxylate to give the carboxylic acid. Thus, neutralization of the IA carboxylate via charge–dipole interactions within a microenvironment that generates an electrostatic field with a net positive charge could account for this shift. Such interactions are known to lower the excitation energy for the  $\pi$ – $\pi^*$  electronic transition of the IA chromophore and shift the absorption maximum to longer wavelengths (Table 4) (47, 48). It is likely that the binding of IA to the  $\beta$ -site mimics the binding of L-Ser or L-Trp. Accordingly, the carboxylate of IA would occupy the same subsite as the negatively charged carboxylates of these substrates, and the indole ring NH group would be H-bonded to the carboxylate of  $\beta$ Glu109 (37). In the E(Aex<sub>1</sub>) structures of either wild-type or T183V mutant tryptophan synthase (e.g., see PDB entry 1KFJ or 1KFE, respectively) (28), the carboxylate of the L-Ser external aldimine is bound at the  $\beta$ -site via a constellation of interactions consisting of the backbone amide NH groups of the  $\beta$ L3 loop,  $\beta$ Gly111,  $\beta$ Gln114, and  $\beta$ His115, the side chain hydroxyl of  $\beta$ Thr110, and a water molecule. All of these H-bond donors are bonded to the oxygens of the E(Aex<sub>1</sub>) carboxylate group. Apparently, the dipolar interactions provided by these groups are sufficient to neutralize the charge on the L-Ser carboxylate. The structure of the complex formed with F9 and IA is consistent with the IA carboxylate inserted into this site. Therefore, these interactions would neutralize the IA carboxylate charge and perturb the electron density distribution over the IA  $\pi$ -system.

**Mechanism of the ASL-Mediated Binding of IA to the  $\beta$ -Site.** The results presented in Figures 1–6 establish that



ASLs alter the binding of IA to the  $\beta$ -site via heterotropic site–site interactions. The salient features of these binding interactions are summarized below.

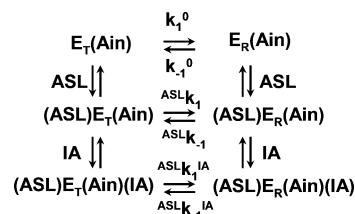
(1) The absorption spectrum of IA bound to the  $\beta$ -site of E(Ain) is red-shifted when G3P or IGP analogues such as GP (Figure 1), F9, and F6 bind to the  $\alpha$ -site, and the affinity for IA is increased (Table 1). The red shift in the absorption spectrum of IA results from a change in the microenvironment of the IA carboxylate upon binding to the  $\beta$ -site when the  $\alpha$ -site is occupied by an ASL. ASL binding exerts synergistic effects on IA binding that have allosteric origins (Figures 1–6 and Tables 1, 2 and 3). We postulate that this allosteric behavior arises from the effector roles played by ASLs in stabilizing the partially closed and/or fully closed conformations of the  $\beta$ -site, and this allostery mimics the *in vivo* roles proposed for IGP and G3P in the regulation of substrate channeling (16).

(2) At ASL concentrations much greater than the enzyme concentration, the rates of complex formation show a kinetic behavior that is only weakly dependent on the concentration of IA (Figure 6). Provided that the concentration of IA is significantly greater than the site concentration, the observed rates exhibit either no dependence or only a slight increase as the concentration of IA is increased, and these dependencies appear linear over the concentration range that was tested. The kinetic behavior is consistent with a bimolecular binding model (eq 3 and Table 3) where the rate of dissociation dominates the relaxation expression, giving rise to a weak concentration dependence (Figure 6). This weak dependence also is consistent with the assumption that the binding of IA introduces only a small, essentially negligible perturbation of the system, and that the spectral change accompanying the binding of IA serves as an indicator of the allosteric state of the  $\alpha\beta$  dimeric unit of the internal aldimine.

(3) The dependence of the rate of the IA spectral shift on the ASL concentration (Figure 5) is more interesting because it is diagnostic of the allosteric behavior of the system. Initially, the magnitude of  $1/\tau$  decreases as the ASL concentration is increased; then, at higher ligand concentrations,  $1/\tau$  levels off, giving an apparent hyperbolic dependence (Figure 5A, C, E and G). If it is assumed that (a) the conformational transitions are slow, (b) the binding of ligands to the  $\alpha$ - and  $\beta$ -sites is fast relative to the rate of the conformational transition, and (c) the binding of ASLs shifts the distribution of enzyme conformations in favor of the state with a higher affinity for IA, then this behavior can be explained by a mechanism involving an obligatory interconversion of two internal aldimine states (T and R) with different affinities for IA. The binding scheme for a simple system with these characteristics is presented in Scheme 2, where the R and T subscripts designate the high- and low-affinity forms, respectively, of the internal aldimine species,  $E_T(\text{Ain})$  and  $E_R(\text{Ain})$ , each with different  $\alpha$ - and  $\beta$ -site affinities. Because of the different affinities of  $E_T(\text{Ain})$  and  $E_R(\text{Ain})$ , if both the ASL and IA bind more tightly to  $E_R(\text{Ain})$  than to  $E_T(\text{Ain})$ , then the ASL will function as a positive heterotropic effector of  $E_R(\text{Ain})(\text{IA})$  formation.

This model postulates that the dependence of  $1/\tau$  on [ASL] arises from the switching of the enzyme from the lower-affinity species,  $E_T(\text{Ain})$ , which predominates in the absence of the ASL, to the higher affinity species,  $(\text{ASL})E_R(\text{Ain})$ ,

Scheme 2: Equilibria Depicting the Allosteric Effects of ASL Binding on the Affinity of the  $\beta$ -Site for IA<sup>a</sup>



<sup>a</sup> States with a high affinity for IA are designated with the subscript R.

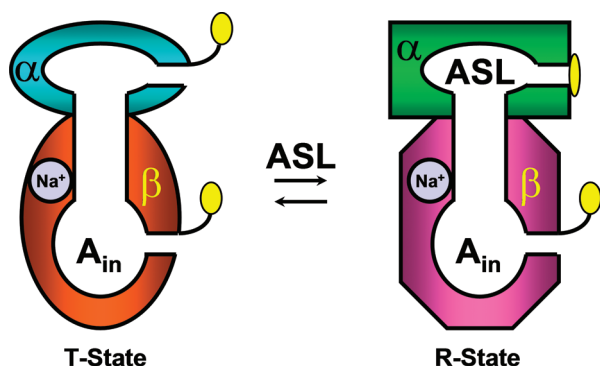
which predominates in the presence of the ASL. As the concentration of the ASL is extrapolated to zero, the expression for  $1/\tau$  simplifies to the sum of the forward and reverse rates for the allosteric transition in the absence of the ASL. At saturating ASL concentrations, the expression for  $1/\tau$  becomes the rate of the forward process for the allosteric transition. Similar behavior has been noted for several other allosteric protein systems, including aspartokinase I-homoserine dehydrogenase, yeast glyceraldehyde-3-phosphate dehydrogenase, and aspartate transcarbamylase (65–68). It has been shown that, provided the conditions stipulated above are valid and provided the ligand concentrations are much greater than the protein site concentrations, the system can be treated as a single conformational transition (68). Consequently, the variation of the concentration of  $E_R(\text{Ain})$  species with time will follow an exponential rate law, and the conformational transition can be described by two apparent rate constants,  $k_1^*$  and  $k_{-1}^*$ , where  $1/\tau = k_1^* + k_{-1}^*$ , corresponding to the weighted averages of the forward and reverse rate constants as defined in Scheme 2. Accordingly,  $k_1^*$  and  $k_{-1}^*$  will vary with the concentration of the allosteric ligand (the ASL in the tryptophan synthase system). This variation will range between two extremes: the value of  $k_1^* + k_{-1}^*$  measured in the absence of the ASL (here designated as  $k_1^0 + k_{-1}^0$ ) and the value of  $k_1^*$  and  $k_{-1}^*$  extrapolated to an infinite concentration of the ASL ( $k_1^{\text{ASL}} + k_{-1}^{\text{ASL}}$ ) (68). Therefore

$$1/\tau = k_{-1}^0 + k_1^0(1 + [\text{ASL}]/K_T)/(1 + [\text{ASL}]/K_R) \quad (4)$$

According to eq 4, the dependence of  $1/\tau$  on [ASL] should extrapolate to a value of  $1/\tau_0 = k_1^0 + k_{-1}^0$  when [ASL] = 0. If  $K_T \gg K_R$ , then  $1/\tau$  simplifies and  $1/\tau_0 = k_{-1}^0$ . The data for GP, F9, F6, and G3P presented in Figure 5 (panels A, C, E, and G, respectively) were fitted to eq 4, and the values of  $k_1^0$ ,  $k_{-1}^0$ ,  $K_T$ , and  $K_R$  obtained from the best fit are listed in Table 2. The ASLs, GP, G3P, and F9 give very similar rate parameters (Table 2), whereas F6 exhibits divergent behavior. It is shown in ref 42 that F6 binding displays some unique features (see below) that might give rise to this difference.

**Structural Evidence for ASL-Dependent Priming.** The comparison of different E(Ain) structures in complex with F6, F9, F19, and different analogues (IGP and IPP) supports the kinetic findings of two different states that exhibit different affinities for the  $\alpha$ - or  $\beta$ -active site. Binding of ASL to the  $\alpha$ -subdomain of the holoenzyme leads to a structuring of the surrounding microenvironment of the  $\alpha$ -active site. As a result of a number of structural rearrangements that are transmitted via a structural “intersubunit communication

Scheme 3: Cartoon Postulating Conformational Changes in the  $\alpha$ - and  $\beta$ -Sites of the Internal Aldimine Resulting from the Binding of ASLs to an  $\alpha\beta$  Dimeric Unit of Tryptophan Synthase<sup>a</sup>



<sup>a</sup> When an ASL binds to the  $\alpha$ -site, loop  $\alpha$ L6 folds down on loop  $\alpha$ L2, forming a lid (yellow) that closes or partially closes the  $\alpha$ -site. The resulting allosteric effect switches the  $\beta$ -subunit from a low-affinity T state to a higher-affinity R state. The R state exhibits a greater affinity for substrates and substrate analogues such as IA.

pathway” consisting of  $\alpha$ L2, and parts of the COMM domain,  $\beta$ 139–142,  $\beta$ 158–181 (including  $\beta$ H6), and  $\beta$ 295–305, the  $\beta$ -active site was found to become structurally more rigid (42). Thereby, the  $\beta$ -active site adopts a conformation that is prepared (“primed”) for L-Ser, or in this case IA, binding thus leading to an increased affinity. The structurally more unstructured (“unprimed”) conformation of the holoenzyme in the absence of an  $\alpha$ -site ligand would correspond to the  $E_T(A_{in})$  low-affinity state, whereas the ordered, primed conformation displays the  $E_R(A_{in})$  high-affinity state of the internal aldimine after ASL binding.

While all new ASLs were shown to bind to the  $\alpha$ -active site, F6 appears to be the most flexible which reflects the experimental results. Its unique structure enables it to adopt slightly different conformations in the active site [observed in the  $E(A_{in})$  and  $E(A_{ex1})$  states] (42, 43). A consequence of its flexibility is that its ability to prime the  $\beta$ -site is weaker than that of F9. Another point is that high concentrations of F6 yielded a structure that displays a second F6 molecule bound at the opening of the tunnel (PDB entry 2CLF). Binding of F6 to this potential secondary binding site was shown to influence the overall rigidity of the structure and might be responsible for noticeable differences observed in the experiments.

The cartoon in Scheme 3 depicts the conformational transitions in the  $\alpha$ - and  $\beta$ -subunits that are postulated to accompany the binding of IGP (or a close analogue of IGP) to the  $\alpha$ -site. According to this scheme, IGP binding (and the binding of close IGP analogues such as GP and F9) switches the  $\alpha$ -site to a semiclosed conformation and favors the conversion of the  $\beta$ -site to a conformation with increased affinity for substrate or substrate analogues such as IA, designated as the R state. According to Schemes 2 and 3, the function of the ASL-mediated allosteric interaction in the  $E(A_{in})$  species is to switch the  $\beta$ -subunit to a conformational state with increased affinity for substrate during the physiological  $\alpha\beta$  reaction. Formation of the  $E(A-A)$  species at the  $\beta$ -active site induces an isomerization of the  $\alpha$ -site to the fully closed, enzymatically active state.

In summary, previous work has shown that the allosteric behavior of the tryptophan synthase system is greatly

dependent upon the covalent state of the  $\beta$ -site; the transformations between  $E(A_{ex1})$  and  $E(A-A)$  and between  $E(Q_3)$  and  $E(A_{ex2})$  play central roles in the allosteric regulation of substrate channeling (4, 9, 16, 17, 26, 27). These allosteric transitions switch the enzyme between open conformations of low activity and closed conformations of high activity. This work demonstrates for the first time that the  $\alpha$ - and  $\beta$ -sites of the internal aldimine form of the tryptophan synthase bienzyme complex switch between allosteric states of low and high affinity in response to binding of ligand at the  $\alpha$ -site. The kinetic analysis presented herein quantifies the allosteric properties of the internal aldimine form of tryptophan synthase. This work also demonstrates the usefulness of the new classes of ASLs, represented by F6 and F9, as probes of allosteric function in tryptophan synthase. Through the use of G3P and ASL analogues of the physiologically relevant substrates, such as GP, F6, and F9, our future work will further explore the mechanism of the allosteric regulation of tryptophan synthase at a detailed structural and kinetic level.

## REFERENCES

1. Kirschner, K., Weischet, W., and Wiskocil, R. L. (1975) Ligand binding to enzyme complexes, in *Protein-Ligand Interactions* (Sund, H., and Blaver, G., Eds.) pp 27–44, Walter de Gruyter, Berlin.
2. Weischet, W. O., and Kirschner, K. (1976) The binding of indole to the  $\alpha$ -subunit and  $\beta$ -subunit and to the  $\alpha\beta$ -complex of tryptophan synthase from *Escherichia coli*. Identification of a second indole-binding site on the  $\alpha$ -subunit, *Eur. J. Biochem.* 64, 313–320.
3. Houben, K. F., and Dunn, M. F. (1990) Allosteric effects acting over a distance of 20–25 Å in the *Escherichia coli* tryptophan synthase bienzyme complex increase ligand affinity and cause redistribution of covalent intermediates, *Biochemistry* 29, 2421–2429.
4. Dunn, M. F., Aguilar, V., Brzovic, P., Drewe, W. F., Jr., Houben, K. F., Leja, C. A., and Roy, M. (1990) The tryptophan synthase bienzyme complex transfers indole between the  $\alpha$ - and  $\beta$ -sites via a 25–30 Å long tunnel, *Biochemistry* 29, 8598–8607.
5. Lane, A. N., and Kirschner, K. (1991) Mechanism of the physiological reaction catalyzed by tryptophan synthase from *Escherichia coli*, *Biochemistry* 30, 479–484.
6. Kirschner, K., Lane, A. N., and Strasser, A. W. M. (1991) Reciprocal communication between the lyase and synthase active sites of the tryptophan synthase bienzyme complex, *Biochemistry* 30, 472–478.
7. Anderson, K. S., Miles, E. W., and Johnson, K. A. (1991) Serine modulates substrate channeling in tryptophan synthase: A novel intersubunit triggering mechanism, *J. Biol. Chem.* 266, 8020–8033.
8. Miles, E. W. (1991) Structural basis for catalysis by tryptophan synthase, *Adv. Enzymol. Relat. Areas Mol. Biol.* 64, 93–172.
9. Brzovic, P. S., Ngo, K., and Dunn, M. F. (1992) Allosteric interactions coordinate catalytic activity between successive metabolic enzymes in the tryptophan synthase bienzyme complex, *Biochemistry* 31, 3831–3839.
10. Brzovic, P. S., Sawa, Y., Hyde, C. C., Miles, E. W., and Dunn, M. F. (1992) Evidence that mutations in a loop region of the  $\alpha$ -subunit inhibit the transition from an open to a closed conformation in the tryptophan synthase bienzyme complex, *J. Biol. Chem.* 267, 13028–13038.
11. Brzovic, P. S., Hyde, C. C., Miles, E. W., and Dunn, M. F. (1993) Characterization of the functional role of a flexible loop in the  $\alpha$ -subunit of tryptophan synthase from *Salmonella typhimurium* by rapid-scanning, stopped-flow spectroscopy and site-directed mutagenesis, *Biochemistry* 32, 10404–10413.
12. Leja, C. A., Woehl, E. U., and Dunn, M. F. (1995) Allosteric linkages between  $\beta$ -site covalent transformations and  $\alpha$ -site activation and deactivation in the tryptophan synthase bienzyme complex, *Biochemistry* 34, 6552–6561.

13. Miles, E. W. (1995) Tryptophan synthase. Structure, function, and protein engineering, *Subcell. Biochem.* 24, 207–254.
14. Peracchi, A., Bettati, S., Mozzarelli, A., Rossi, G. L., Miles, E. W., and Dunn, M. F. (1996) Allosteric regulation of tryptophan synthase: Effects of pH, temperature, and  $\alpha$ -subunit ligands on the equilibrium distribution of pyridoxal 5'-phosphate-L-serine intermediates, *Biochemistry* 35, 1872–1880.
15. Pan, P., and Dunn, M. F. (1996)  $\beta$ -Site covalent reactions trigger transitions between open and closed conformations of the tryptophan synthase bienzyme complex, *Biochemistry* 35, 5002–5013.
16. Pan, P., Woehl, E., and Dunn, M. F. (1997) Protein architecture, dynamics and allostery in tryptophan synthase channeling, *Trends Biochem. Sci.* 22, 22–27.
17. Woehl, E. U., and Dunn, M. F. (1995) Monovalent metal ions play an essential role in catalysis and intersubunit communication in the tryptophan synthase bienzyme complex, *Biochemistry* 34, 9466–9476.
18. Woehl, E., and Dunn, M. F. (1999) Mechanisms of monovalent cation action in enzyme catalysis: The first stage of the tryptophan synthase  $\beta$ -reaction, *Biochemistry* 38, 7118–7130.
19. Woehl, E., and Dunn, M. F. (1999) Mechanisms of monovalent cation action in enzyme catalysis: The tryptophan synthase  $\alpha$ -,  $\beta$ -, and  $\alpha\beta$ -reactions, *Biochemistry* 38, 7131–7141.
20. Rowlett, R., Yang, L. H., Ahmed, S. A., McPhie, P., Jhee, K. H., and Miles, E. W. (1998) Mutations in the contact region between the  $\alpha$  and  $\beta$  subunits of tryptophan synthase alter subunit interaction and intersubunit communication, *Biochemistry* 37, 2961–2968.
21. Schneider, T. R., Gerhardt, E., Lee, M., Liang, P. H., Anderson, K. S., and Schlichting, I. (1998) Loop closure and intersubunit communication in tryptophan synthase, *Biochemistry* 37, 5394–5406.
22. Miles, E. W., Rhee, S., and Davies, D. R. (1999) The molecular basis of substrate channeling, *J. Biol. Chem.* 274, 12193–12196.
23. Bahar, I., and Jernigan, R. L. (1999) Cooperative fluctuations and subunit communication in tryptophan synthase, *Biochemistry* 38, 3478–3490.
24. Marabotti, A., Cozzini, P., and Mozzarelli, A. (2000) Novel allosteric effectors of the tryptophan synthase  $\alpha_2\beta_2$  complex identified by computer-assisted molecular modeling, *Biochim. Biophys. Acta* 1476, 287–299.
25. Marabotti, A., De, B. D., Tramonti, A., Bettati, S., and Mozzarelli, A. (2001) Allosteric communication of tryptophan synthase. Functional and regulatory properties of the  $\beta$  S178P mutant, *J. Biol. Chem.* 276, 17747–17753.
26. Weber-Ban, E., Hur, O., Bagwell, C., Banik, U., Yang, L. H., Miles, E. W., and Dunn, M. F. (2001) Investigation of allosteric linkages in the regulation of tryptophan synthase: The roles of salt bridges and monovalent cations probed by site-directed mutation, optical spectroscopy, and kinetics, *Biochemistry* 40, 3497–3511.
27. Harris, R. M., and Dunn, M. F. (2002) Intermediate trapping via a conformational switch in the  $\text{Na}^+$ -activated tryptophan synthase bienzyme complex, *Biochemistry* 41, 9982–9990.
28. Kulik, V., Weyand, M., Seidel, R., Niks, D., Arac, D., Dunn, M. F., and Schlichting, I. (2002) On the role of  $\alpha\text{Thr183}$  in the allosteric regulation and catalytic mechanism of tryptophan synthase, *J. Mol. Biol.* 324, 677–690.
29. Weyand, M., Schlichting, I., Marabotti, A., and Mozzarelli, A. (2002) Crystal structures of a new class of allosteric effectors complexed to tryptophan synthase, *J. Biol. Chem.* 277, 10647–10652.
30. Weyand, M., Schlichting, I., Herde, P., Marabotti, A., and Mozzarelli, A. (2002) Crystal structure of the  $\beta\text{Ser178} \rightarrow \text{Pro}$  mutant of tryptophan synthase. A “knock-out” allosteric enzyme, *J. Biol. Chem.* 277, 10653–10660.
31. Osborne, A., Teng, Q., Miles, E. W., and Phillips, R. S. (2003) Detection of open and closed conformations of tryptophan synthase by  $^{15}\text{N}$ -heteronuclear single-quantum coherence nuclear magnetic resonance of bound L- $^{15}\text{N}$ -tryptophan, *J. Biol. Chem.* 278, 44083–44090.
32. Phillips, R. S., Miles, E. W., Holtermann, G., and Goody, R. S. (2005) Hydrostatic pressure affects the conformational equilibrium of *Salmonella typhimurium* tryptophan synthase, *Biochemistry* 44, 7921–7928.
33. Harris, R. M., Ngo, H., and Dunn, M. F. (2005) Synergistic effects on escape of a ligand from the closed tryptophan synthase bienzyme complex, *Biochemistry* 44, 16886–16895.
34. Hyde, C. C., Ahmed, S. A., Padlan, E. A., Miles, E. W., and Davies, D. R. (1988) Three-dimensional structure of the tryptophan synthase  $\alpha_2\beta_2$  multienzyme complex from *Salmonella typhimurium*, *J. Biol. Chem.* 263, 17857–17871.
35. Rhee, S., Parris, K. D., Ahmed, S. A., Miles, E. W., and Davies, D. R. (1996) Exchange of  $\text{K}^+$  or  $\text{Cs}^+$  for  $\text{Na}^+$  induces local and long-range changes in the three-dimensional structure of the tryptophan synthase  $\alpha_2\beta_2$  complex, *Biochemistry* 35, 4211–4221.
36. Rhee, S., Miles, E. W., and Davies, D. R. (1998) Cryo-crystallography of a true substrate, indole-3-glycerol phosphate, bound to a mutant ( $\alpha\text{D60N}$ ) tryptophan synthase  $\alpha_2\beta_2$  complex reveals the correct orientation of active site  $\alpha\text{Glu49}$ , *J. Biol. Chem.* 273, 8553–8555.
37. Rhee, S., Parris, K. D., Hyde, C. C., Ahmed, S. A., Miles, E. W., and Davies, D. R. (1997) Crystal structures of a mutant ( $\beta\text{K87T}$ ) tryptophan synthase  $\alpha_2\beta_2$  complex with ligands bound to the active sites of the  $\alpha$ - and  $\beta$ -subunits reveal ligand-induced conformational changes, *Biochemistry* 36, 7664–7680.
38. Sachpatzidis, A., Dealwis, C., Lubetsky, J. B., Liang, P. H., Anderson, K. S., and Lolis, E. (1999) Crystallographic studies of phosphonate-based  $\alpha$ -reaction transition-state analogues complexed to tryptophan synthase, *Biochemistry* 38, 12665–12674.
39. Kulik, V., Hartmann, E., Weyand, M., Frey, M., Gierl, A., Niks, D., Dunn, M. F., and Schlichting, I. (2005) On the structural basis of the catalytic mechanism and the regulation of the  $\alpha$  subunit of tryptophan synthase from *Salmonella typhimurium* and BX1 from maize, two evolutionarily related enzymes, *J. Mol. Biol.* 352, 608–620.
40. Yanofsky, C., and Crawford, I. P. (1972) Tryptophan Synthase, in *The Enzyme* (Boyer, P. D., Ed.) 3rd ed., pp 1–31, Academic Press, New York.
41. Miles, E. W. (1979) Tryptophan synthase: Structure, function, and subunit interaction, *Adv. Enzymol. Relat. Areas Mol. Biol.* 49, 127–186.
42. Ngo, H., Harris, R., Kimmich, N., Casino, P., Niks, D., Blumenstein, L., Barends, T. R., Kulik, V., Weyand, M., Schlichting, I., and Dunn, M. F. (2007) Synthesis and characterization of allosteric probes of substrate channeling in the tryptophan synthase bienzyme complex, *Biochemistry* 46, 7713–7727.
43. Ngo, H., Kimmich, N., Harris, R., Niks, N., Blumenstein, L., Kulik, V., Barends, T. R., Schlichting, I., and Dunn, M. F. (2007) Allosteric regulation of substrate channeling in tryptophan synthase: modulation of the L-serine reaction in stage I of the  $\beta$ -reaction by  $\alpha$ -site ligands, *Biochemistry* 46, 7740–7753.
44. Miles, E. W., Bauerle, R., and Ahmed, S. A. (1987) Tryptophan synthase from *Escherichia coli* and *Salmonella typhimurium*, *Methods Enzymol.* 142, 398–414.
45. Metzler, C. M., Cahill, A. E., Petty, S., Metzler, D. E., and Lang, L. (1985) The widespread applicability of lognormal curves for the description of absorption-spectra, *Appl. Spectrosc.* 39, 333–339.
46. Bernasconi, C. (1976) *Relaxation Kinetics*, Academic Press, New York.
47. Charney, E., and Bernhard, S. A. (1967) Optical properties and chemical nature of acyl-chymotrypsin linkages, *J. Am. Chem. Soc.* 89, 2726–2733.
48. Angelis, C. T., Dunn, M. F., Muchmore, D. C., and Wing, R. M. (1977) Lewis acid complexes which show spectroscopic similarities to an alcohol-dehydrogenase ternary complex, *Biochemistry* 16, 2922–2931.
49. Buckley, P. D., and Dunn, M. F. (1982) Observation of acyl-enzyme intermediates in the sheep liver aldehyde dehydrogenase catalytic mechanism via rapid-scanning UV-visible spectroscopy, *Prog. Clin. Biol. Res.* 114, 23–35.
50. Dunn, M. F., and Buckley, P. D. (1985) Kinetic and spectroscopic characterization of the sheep liver aldehyde dehydrogenase acyl-enzyme, *Prog. Clin. Biol. Res.* 174, 15–27.
51. Bender, M. L., Zerner, B., and Schonbaum, G. R. (1962) Spectrophotometric investigations of mechanism of  $\alpha$ -chymotrypsin-catalyzed hydrolyses: Detection of acyl-enzyme intermediate, *J. Am. Chem. Soc.* 84, 2540–2550.
52. Bender, M. L., and Zerner, B. (1962) Formation of an acyl-enzyme intermediate in  $\alpha$ -chymotrypsin-catalyzed hydrolyses of non-labile trans-cinnamic acid esters, *J. Am. Chem. Soc.* 84, 2550–2556.
53. Bernhard, S. A., and Tashjian, Z. H. (1965) Acyl intermediates in  $\alpha$ -chymotrypsin-catalyzed hydrolysis of indoleacryloylimidazole, *J. Am. Chem. Soc.* 87, 1806–1811.



54. Bernhard, S. A., Lau, S. J., and Noller, H. (1965) Spectrophotometric identification of acyl enzyme intermediates, *Biochemistry* 4, 1108–1118.
55. Henderson, R. (1970) Structure of crystalline  $\alpha$ -chymotrypsin. IV. The structure of indoleacryloyl- $\alpha$ -chymotrypsin and its relevance to the hydrolytic mechanism of the enzyme, *J. Mol. Biol.* 54, 341–354.
56. Bernhard, S. A., and Lau, S. (1972) Spectrophotometric and structural evidence as to the mechanism of protease catalysis at chemical bonding resolution, *Cold Spring Harbor Symp. Quant. Biol.* 36, 75–83.
57. Dunn, M. F., and Bernhard, S. A. (1969) Conjugate addition to activated  $\beta$ -arylacrylic acid derivatives. Thiolate anions, *J. Am. Chem. Soc.* 91, 3274–3280.
58. Malhotra, O. P., and Bernhard, S. A. (1968) Spectrophotometric identification of an active site-specific acyl glyceraldehyde 3-phosphate dehydrogenase: Regulation of its kinetic and equilibrium properties by coenzyme, *J. Biol. Chem.* 243, 1243–1254.
59. Dunn, M. F., and Hutchison, J. S. (1973) Roles of zinc ion and reduced coenzyme in formation of a transient chemical intermediate during equine liver alcohol-dehydrogenase catalyzed reduction of an aromatic aldehyde, *Biochemistry* 12, 4882–4892.
60. Dunn, M. F., Dietrich, H., Macgibbon, A. K. H., Koerber, S. C., and Zeppezauer, M. (1982) Investigation of intermediates and transition-states in the catalytic mechanisms of active-site substituted cobalt(II), nickel(II), zinc(II), and cadmium(II) horse liver alcohol-dehydrogenase, *Biochemistry* 21, 354–363.
61. Dahl, K. H., and Dunn, M. F. (1984) Reaction of 4-trans-(N,N-dimethylamino)cinnamaldehyde with the liver alcohol dehydrogenase-oxidized nicotinamide adenine-dinucleotide complex, *Biochemistry* 23, 4094–4100.
62. Dahl, K. H., and Dunn, M. F. (1984) Carboxymethylated liver alcohol dehydrogenase: Kinetic and thermodynamic characterization of reactions with substrates and inhibitors, *Biochemistry* 23, 6829–6839.
63. McFarland, J. T., Lee, M. Y., Reinsch, J., and Raven, W. (1982) Reactions of  $\beta$ -(2-furyl) propionyl coenzyme-A with general fatty acyl-CoA dehydrogenase, *Biochemistry* 21, 1224–1229.
64. Qin, L., and Srivastava, D. K. (1998) Energetics of two-step binding of a chromophoric reaction product, trans-3-indoleacryloyl-CoA, to medium-chain acyl-coenzyme-A dehydrogenase, *Biochemistry* 37, 3499–3508.
65. Kirschner, K., Eigen, M., Bittman, R., and Voigt, B. (1966) Binding of nicotinamide-adenine dinucleotide to yeast D-glyceraldehyde-3-phosphate dehydrogenase: Temperature-jump relaxation studies on mechanism of an allosteric enzyme, *Proc. Natl. Acad. Sci. U.S.A.* 56, 1661–1666.
66. Eigen, M. (1967) Kinetics of reaction control and information transfer in enzymes and in nucleic acids, in *Nobel Symposium* (Claesson, Ed.) pp 333–339, Almquist and Wiksell, Stockholm.
67. Hammes, G. G., and Wu, C. W. (1971) Relaxation spectra of aspartate transcarbamylase: Interaction of native enzyme with aspartate analogs, *Biochemistry* 10, 1051–1057.
68. Janin, J. (1971) Relaxation studies on an allosteric enzyme: Aspartokinase I-homoserine dehydrogenase-I, *Cold Spring Harbor Symp. Quant. Biol.* 36, 193–198.

BI700386B